Laser and Particle Beams, page 1 of 10, 2012.

doi:10.1017/S0263034611000851

Modified wire array underwater electrical explosion

L. GILBURD, S. EFIMOV, A. FEDOTOV GEFEN, V. TZ. GUROVICH, G. BAZALITSKI, O. ANTONOV, AND YA. E. KRASIK

Physics Department, Technion, Haifa, Israel

(RECEIVED 5 October 2011; ACCEPTED 16 November 2011)

Abstract

The results of experiments involving underwater electrical explosion of different wire arrays using an outer metallic cylinder as a shock reflector are presented. A pulse generator with a stored energy of about 6 kJ, current amplitude ≤ 500 kA, and rise time of 350 ns was used for the wire array explosion. The results of the experiments and of hydrodynamic simulations showed that in the case of a Cu wire array explosion, the addition of the reflector increases the pressure and temperature of the water in the vicinity of the implosion axis about 1.38 and about 1.33 times, respectively. Also, it was shown that in the case of an Al wire array explosion with stainless steel reflector, Al combustion results, and, accordingly, additional energy is delivered to the converging water flow generating about 540 GPa pressure in the vicinity of the explosion axis. Finally, it was found that microsecond time scale light emission that appears with microsecond time scale delay with respect to the nanosecond time scale self-light emission of the compressed water in the vicinity of the implosion axis is related to water bubbles formation which scattered light of exploded wires.

Keywords: Electrical wire explosion; Strong shock wave; Warm dense plasma

1. INTRODUCTION

The results of recent research (Krasik *et al.*, 2007; Grinenko *et al.*, 2007; Fedotov *et al.*, 2007; Fedotov-Gefen *et al.*, 2010, 2011) on underwater electrical wire array explosions showed that this method can be considered as an alternative to that using light gas guns (Mitchell & Nellis, 1981), *Z*-pinch (Spielman *et al.*, 1998), powerful lasers (Celliers *et al.*, 2004; Kolacek *et al.*, 2010), or intense heavy ion beams (Tahir *et al.*, 2010) to form warm dense matter (Sasaki *et al.*, 2006). In addition, this method can be especially useful for studying water in extreme states, which is important for studying the physics of giant planets (Lindl *et al.*, 1995; Nellis *et al.*, 1997; Goldman *et al.*, 2009). Indeed, experimental data coupled with hydrodynamic simulations (HD) showed that the efficiency of the energy transfer from the exploding wires to the generated water flow is $20 \pm 4\%$ (Grinenko *et al.*, 2006; Efimov *et al.*, 2009). This allows one to consider that in the case of cylindrical wire array explosion about 10% of the energy deposited into the exploding wires is delivered to the converging water flow. Experimental results (Fedotov *et al.*, 2007) showed that the electrical explosion of a cylindrical wire array is accompanied by the generation of a converging strong shock wave (SSW) that is formed as a result of the overlapping of SSWs formed by radially expanding exploding wires. It was shown that this converging SSW retains its azimuthal and longitudinal symmetry up to a Mach number of 12. In the vicinity of the implosion axis, this converging SSW forms an extreme state of water with density up to about 4 g/cm^3, temperature of about 10^4 K, and pressure up to 400 GPa when a submicrosecond generator with stored energy of about 8 kJ is used (Fedotov-Gefen *et al.*, 2011).

In this paper, are reported the results of experimental research and HD simulations of the increase in the pressure, density, and temperature of the "water" in the vicinity of the implosion axis when the same pulsed generator as in Fedotov-Gefen *et al.* (2011), but a modified cylindrical wire array design are used in the underwater electric explosion. That is, in this set of experiments, an outer metallic cylinder was used to produce a reflection of the SSW expanding outward from the exploding wire array. This SSW, which is reflected from the outer cylinder, increases significantly the energy delivered to the converging part of the water flow and, respectively, the density, temperature, and pressure of water in the vicinity of the implosion axis.

Address correspondence and reprint requests to: Yakov E. Krasik, Physics Department, Technion 32000 Haifa, Israel. E-mail: fnkrasik@physics.technion.ac.il

2. EXPERIMENTAL SETUP

The experimental setup is shown in Figure 1. A high-current sub-microsecond time scale generator (Kovalchuk *et al.*, 2009) with stored energy up to 9.6 kJ at a charging voltage of 100 kV delivers a current pulse with an amplitude of 760 kA and rise time of 400 ns to a 17 nH inductive load. The discharged voltage and current (see Fig. 2) were measured using a calibrated capacitive voltage divider and two B-dot probes, respectively. The wire array was placed between the high-voltage and grounded electrodes, which were immersed in de-ionized water (total volume of 0.4 L). The experiments with wire array electrical explosions were carried out at a generator charging voltage and stored energy of 80 kV and 6.14 kJ, respectively.

During the wire array explosion, a half of the generated water flow propagates outward from the wire array. In order to reflect a part of this diverging energy back toward the array axis, an outer cylinder made of duralumin with a density of about 2.7 g/cm^3 was used as an SSW reflector (see Fig. 3). The inner radius of the reflectors was larger than the array radius by Δr, varied in the range of 0.2–1.5 mm. Namely, in experiments with wire arrays having a radius of 2.5 mm, reflectors with inner radii in the range 2.7–4 mm were used. In order to avoid the electrical breakdown of the gap between the wires and the reflector, the former was coated with a 100 μm thick layer of Al_2O_3.

The parameters of the compressed water in the vicinity of the implosion axis were studied using SSW propagation trajectory, obtained by shadow SSW imaging, and the implosion time, defined by the fast increase of water self-light emission (see Fig. 4). The experimental chamber (see Fig. 1) has two optical windows. The upper window was used for the axial alignment of the system using a CW laser (532 nm, 15 mW) and for backlighting shadow images. The bottom optical window was used to collect the backlighting laser beam and water self-light emission. Interference filters separated the laser light from the light emitted from the water (see Fig. 1). In the green channel (532 nm), a sequence of overlapping shadow images was obtained using a 4QuikE camera with a frame duration ≤10 ns and time delay between frames of 300 ns.

The self-light emission from a small volume of water in the vicinity of the implosion axis was registered by a photo-multiplier tube (PMT) coupled to a 656 nm narrow-band interference filter. Prior to each experiment, the optical system's sensitivity was calibrated using an Oriel QTH200 lamp. The radial cross-section of the observed area was about 1 mm in diameter; the latter was defined by the iris diaphragm I1 (see Fig. 1). The aperture of the iris diaphragm was adjusted to block the light emitted by the exploding wires. In addition, in the case of a wire array that was 5 mm in diameter, in order to avoid scattered light emission from the exploding wires, a thin (0.4 mm) black dielectric

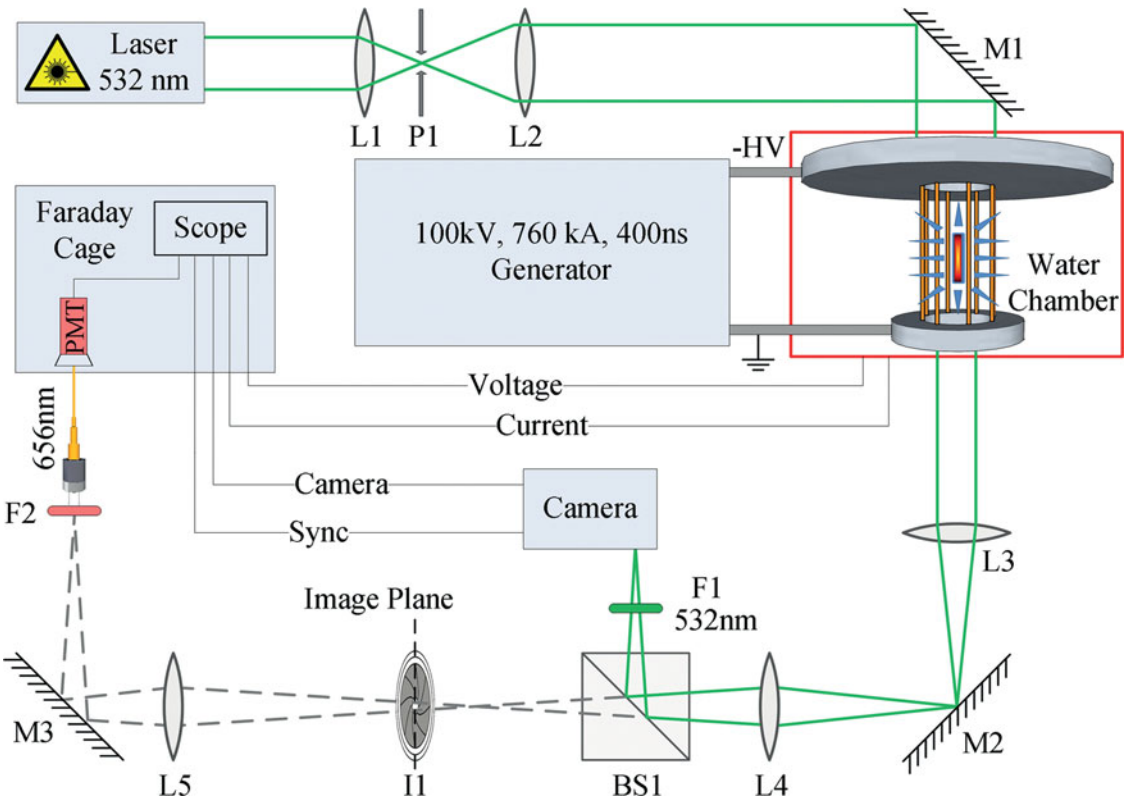

Fig. 1. (Color online) Experimental setup. L1-L5 are the lenses, F1-F2 are the interference filters, M1-M3 are the mirrors, BS1 is the beam splitter, P1 is the pinhole and I1 is the iris diaphragm.

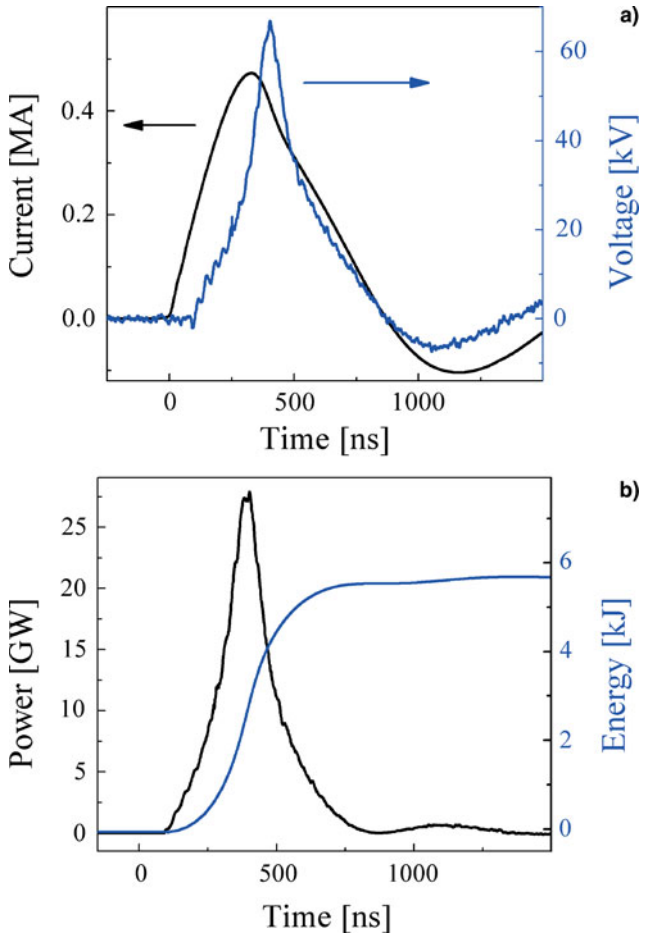

Fig. 2. (Color online) (**a**) Typical waveforms of the discharge current and voltage for charging voltage of the generator of 80 kV. (**b**) Time evolution of the power and energy of 40 Cu wires array electrical explosion.

tube, about 4 mm in diameter, was inserted coaxially inside the array. The time resolution of the red (656 nm) channel was defined by the rise time of the PMTs (about 2 ns). In these experiments, the measurements of the Plank temperature of the self-light emission were not carried out because, as was shown in Fedotov-Gefen *et al.* (2011), the strong bremsstrahlung absorption by colder outer plasma layers in the vicinity of the implosion axis does not allow one to determine the temperature in the inner "water" layers.

3. EXPERIMENTAL RESULTS

In the present experiments with wire array explosions, the Cu and Al wires diameters were adjusted in such a way that the deposited energy and its deposition rate into the wires were almost identical in both cases. The optimal distance between the wire array and the reflector for each array diameter was chosen according to the HD simulation results, which will be described in the Section 4.2. Here let us note that when the duralumin reflector was placed at $\Delta r \leq 0.5$ mm, a small increase in the amplitude and ringing of the discharge current and a decrease in the deposited power were obtained (see

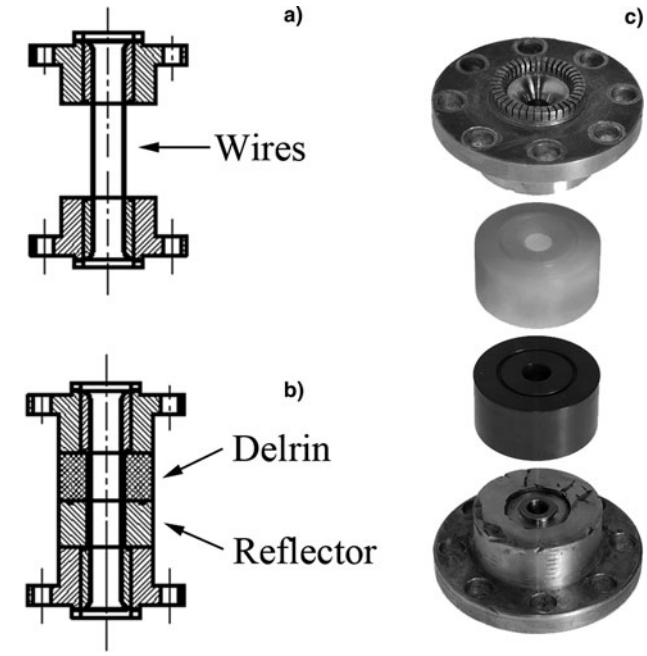

Fig. 3. Different configurations of array: (**a**) array without outer cylinder; (**b**) array with a duralumin made cylinder placed at the bottom half of the array (the ground electrode) and delrin cylinder placed near the HV electrode; (**c**) Parts of the array assembly.

Fig. 5). This effect could be explained by a partial electrical breakdown occurred between the exploding wires and reflector. This breakdown leads to about 15% decrease in the total deposited energy during the first 600 ns of the discharge. At present we do not know what part of the discharge current is switched to the reflector from the exploding wire array, and additional measures are being planned to avoid this effect.

The waveform of self-light emission and the sequence of two SSW front shadow images with a time delay of about

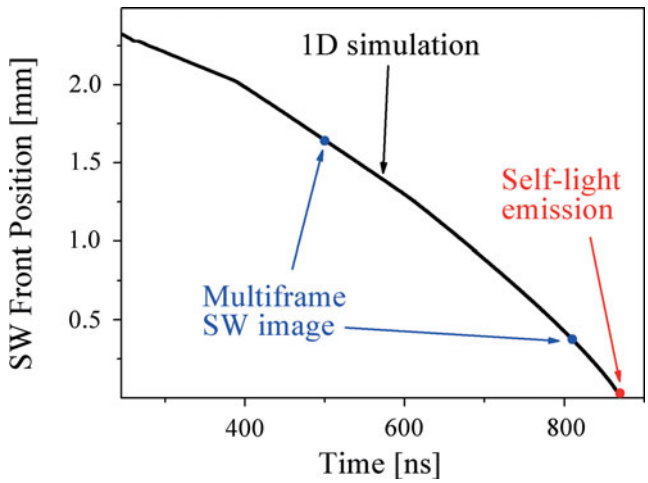

Fig. 4. (Color online) Experimentally obtained and simulated SW propagation with respect to the beginning of the discharge current. Two data points are obtained by overlapping frame images (frame duration of 5 ns and time delay of 300 ns between frames). Underwater electrical explosion of Cu wire array 5 mm in diameter. Zero time is the beginning of the discharge current.

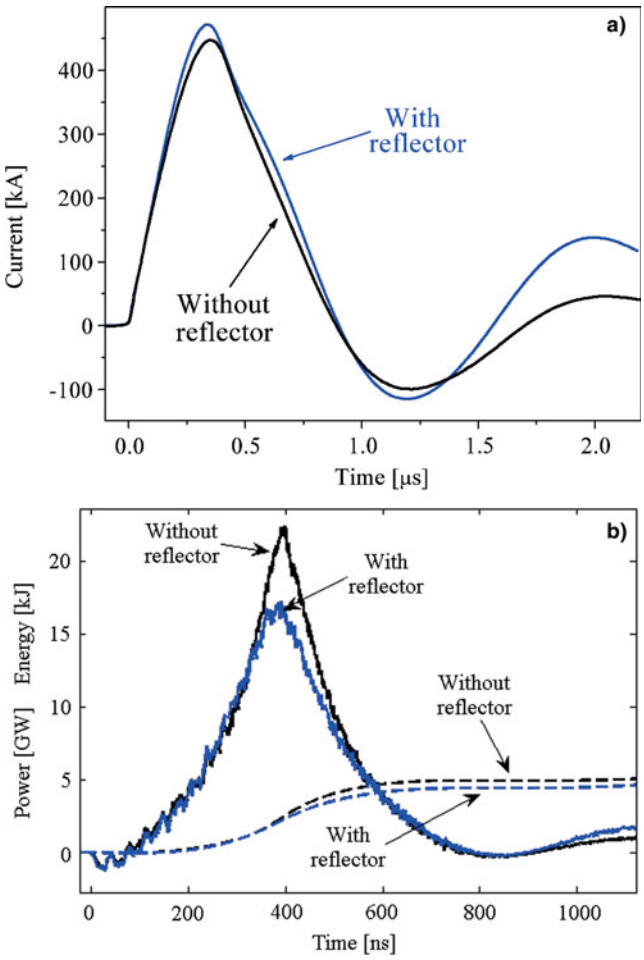

Fig. 5. (Color online) (**a**) Typical waveforms of the discharge currents and (**b**) the deposited power (solid line) and energy (dashed line) in the case of Cu wire array explosion with and without a duralumin reflector. The radial distance between the reflector and the wire array is 0.2 mm. In both experiments, arrays having a diameter of 5 mm were used.

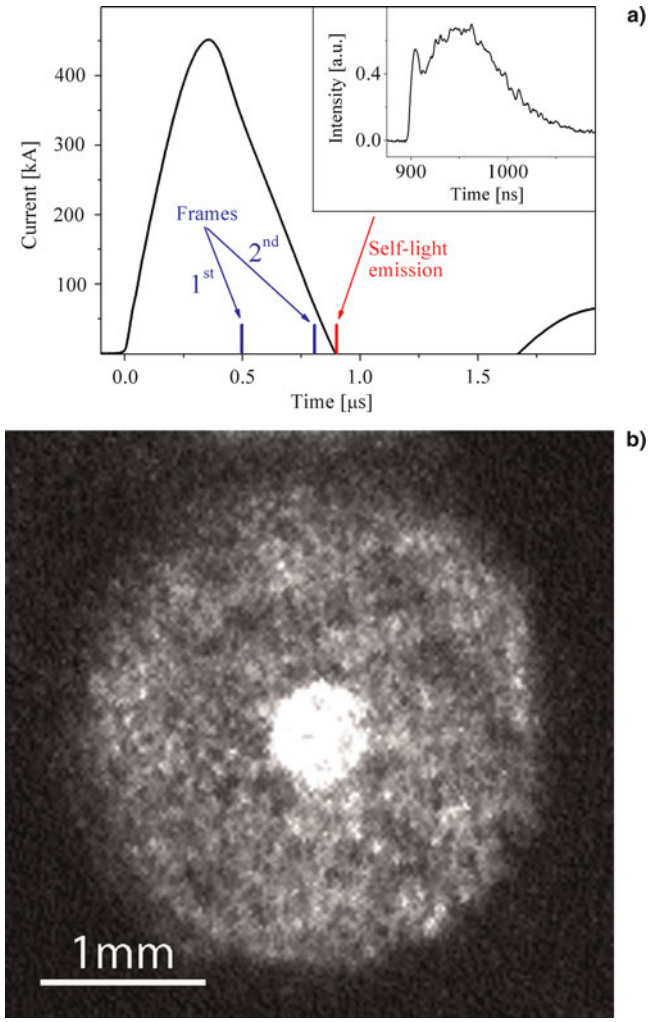

Fig. 6. (Color online) (**a**) Waveform of self-light emission of water in the vicinity of the implosion axis. (**b**) Sequence of two SSW front shadow overlapping images (frame duration of 5 ns) with time delay of about 300 ns between the frames for the explosion of the 5 mm diameter Cu wire array.

300 ns between the frames are shown in Figure 6. One can see that the SSW front has a good azimuthal symmetry. These shadow images, together with the time of the SSW implosion, were used for fitting with the results of the one dimension (1D) HD simulations described in Fedotov-Gefen *et al.* (2011) and Bazalitski *et al.* (2011).

The data of the converging SSW time of flight (TOF) for Cu and Al wire arrays of different diameters, with and without the reflector, are presented in Table 1. Here each TOF data point is an averaged value taken from several (2–3) explosions in identical conditions and it presents the time delay between the beginning of the discharge current and start of the sharp increase in the self-light emission from the water in the vicinity of the implosion axis. One can see that the application of the reflector with $\Delta r = 0.2$ mm and $\Delta r = 0.5$ mm to Cu wire arrays with a diameter of 5 mm and 10 mm, respectively, lead to a shorter implosion time (see Table 1). Namely, the implosion time was decreased by 20 ns and 30 ns for array diameters of 5 mm and 10 mm, respectively. Let us note here, that in the array explosion with the reflector, a decrease in the SSW TOF value was obtained in spite of the lower power and smaller energy deposited into the discharge (see Fig. 5). Thus, one can conclude qualitatively that at least part of the energy of the diverging SSW was reflected from the reflector and delivered to the converging SSW leading to a higher pressure at the SSW front and, respectively, the generation of higher pressure, density, and temperature in the vicinity of the implosion axis. Here let us note that the same experiments using reflectors made of delrin did not show any decrease in the SSW TOF value. In addition, when the duralumin reflector was placed at $\Delta r \geq 1$ mm, a decrease in the SSW TOF was also not obtained.

It is worth mentioning that the reflector consists of two parts (see Fig. 3), the bottom part made of duralumin and the upper part made of delrin. The latter was used as an insulator to avoid electrical breakdown between the high-voltage electrode and the duralumin reflector. The low density of delrin ($1.3\ \mathrm{g/cm^3}$), relative to that of duralumin, causes

Table 1. *Averaged time of the SSW implosion in explosions of Cu wire arrays with diameters of 5 mm and 10 mm and an Al wire array with a diameter of 5 mm*

Cu wires, D = 5 mm		Al wires, D = 5 mm		Cu wires, D = 10 mm	
—	Δr=0.2 mm	—	Δr = 0.2 mm	—	Δr = 0.5 mm
No reflector	With reflector	No reflector	With reflector	No reflector	With reflector
903 ± 6 ns	880 ± 7 ns	822 ± 5 ns	807 ± 5 ns	1.81 ± 0.02 μs	1.78 ± 0.01 μs

only minor changes in the SSW profile according to previous experiments. Therefore, the observed instance of light emission in the vicinity of the implosion axis is related to the "bottom" part of the SSW being affected by the duralumin reflector, i.e., by the reflection of the diverging SSW from the reflector.

To conclude this section, let us note the result of the Al wire array explosion with the duralumin reflector: the SSW TOF had the smallest value (see Table 1). The qualitative explanation of this result is the additional energy delivered to the converging water flow due to the chemical combustion of the Al. An additional decrease in the SSW TOF (down to 795 ± 2 ns) was obtained in Al wire array explosions with a stainless steel reflector. These results will be discussed in Sections 4.1 and 4.2.

4. SIMULATIONS RESULTS

4.1. Simulations' Results of Cu and Al Wire Array Explosions

The 1D HD simulations were based on the code described in Fedotov-Gefen *et al.* (2011) and Bazalitski *et al.* (2011) with some modifications. The issue of the consistency of 1D dimension assumption was addressed in Fedotov *et al.* (2007), where results of two-dimensional (2D) and 1D HD simulations are presented and where it was also demonstrated that, in the case of arrays with a large number of wires (>20), 1D calculations can be successfully employed for numerical analysis. In the present simulation, an axially symmetric water flow is described by the Euler equations in the Lagrange form. The mass of each cylindrical layer is defined as $dm = 2\pi\rho r dr$ where ρ is the water density. The coordinate *r(t,m)* is defined by the Euler equations as

$$\frac{\partial r}{\partial t} = V,\ \frac{\partial r^2}{\partial m} = \frac{1}{\pi\rho}. \tag{1}$$

The motion equation and internal energy conservation law read

$$\frac{\partial V}{\partial t} = -2\pi r\frac{\partial P}{\partial t},\ \frac{\partial \varepsilon}{\partial t} + P\frac{\partial}{\partial t}\left(\frac{1}{\rho}\right) = 0, \tag{2}$$

where *V, P* are the radial velocity and pressure of the water flow, respectively. To calculate the pressure P(ρ, *T*) and internal energy density ε(ρ, *T*), the SESAME equation of state (EOS) database (Lyon & Johnson, 1992) was used. The system of Eqs. (1) and (2) was solved numerically, according to the cross scheme described in Kalitkin (1978).

In the present modified simulations, the SSW generation and propagation velocity were governed not by a converging piston with some defined time-dependent velocity, but by the expansion of a 1D cylindrical "Cu layer" having the same total mass as the exploded wires into which electrical energy was deposited. The entire simulated volume was divided into the following parts: water layer inside the wire array, the exploding "Cu layer," the water layer that occupied the volume between the "Cu layer" and the duralumin reflector, and the reflector layer. The deposition of the energy into the exploding layer was calculated as

$$\frac{dW}{dt} = \alpha\frac{V_\Omega I}{M_{wires}}dm, \tag{3}$$

where V_Ω and *I* are the experimentally obtained resistive voltage and discharge current, respectively, and $\alpha < 1$ is the fitting coefficient. The space Lagrangian cells were chosen to obtain a radius of 2.5 μm for the element adjacent to the axis at the moment of its maximum compression. HD simulations were coupled with the SESAME database of EOS (Lyon & Johnson, 1992) for water, Cu, and Al. Thus, the only fitting parameter was coefficient α, which was adjusted to obtain the best fit between the simulated SSW trajectory and the experimentally obtained SSW TOF data points. In addition, it was checked that the total energy deposited into the converging water flow is ≤ 12%.

The parameters of the SSW reflected from the duralumin reflector were numerically simulated with the application of the SESAME EOS database for Al. The latter allows one to account correctly for the reflector's density depending on the pressure behind the front of the SSW propagating through the reflector. The results of these simulations (the "water" pressure, density, and temperature at $r = 2.5$ μm at the instant of maximum pressure), which use the experimentally measured power deposited into the wire array as the input data and SSW TOF data, are presented in Table 2. In addition, the efficiency of the transfer of the energy deposited into the exploding wire to the energy of the converging water is presented in the last row of Table 2. The errors in the data in Table 2 result from the statistics of several successful explosion shots for each wire array configuration.

Table 2. *Results of simulated values of pressure, density and temperature at* r = *2.5 μm at the implosion axis at the implosion moment when the maximum value of the pressure is realized*

	Cu wires D = 5 mm		Al wires D = 5 mm		Cu wires D = 10 mm	
Reflector	No	Yes	No	Yes	No	Yes
Pressure [GPa]	320 ± 10	444 ± 10	429 ± 15	475 ± 15	190 ± 10	257 ± 10
Density [g/cm^3]	3.78 ± 0.02	4.03 ± 0.02	4.04 ± 0.03	4.13 ± 0.03	3.3 ± 0.04	3.58 ± 0.02
Temperature [eV]	2.08 ± 0.05	2.76 ± 0.05	2.77 ± 0.05	3.03 ± 0.06	1.17 ± 0.06	1.67 ± 0.03
Efficiency [%]	8.6 ± 1	15 ± 1	14.5 ± 1	21.2 ± 2	12 ± 1	20 ± 1.5

The results of the simulations showed that the application of the duralumin reflector leads to an increase in the energy of about 170 J delivered to the converging water flow by the SSW reflected from the reflector. The latter leads to an increase in the values of pressure, density, and temperature at $r = 2.5$ μm by 38%, 7%, and 33%, respectively, in case of the Cu array with a diameter of 5 mm, and by 35%, 8%, and 43% in case of the Cu array with a diameter of 10 mm. In addition, one can see a significant increase in the efficiency of the energy transfer to the generated converging water flow. Here, let us remember once more that when a reflector was used, there was about a 15% decrease in the energy deposited into the wires. In spite of this, one can see a significant increase in the pressure (energy density) in the vicinity of the implosion axis.

The experimental and simulation results showed, in accord with theoretical predictions, that the application of the reflector allows one to increase significantly the time duration and volume of the highly compressed water. The time dependence of the radial position of a pressure of 100 GPa in the water is shown in Figure 7. One can see that when the reflector is applied, the volume of water with this pressure increases about 3.4 times and the duration of this pressure in the water increases about 1.75 times.

In Table 2, one can see that the results of the simulations of the Al wire array without the duralumin reflector showed almost the same values of pressure, density, and temperature as those of the Cu wire array explosion with the reflector, in spite of the significantly shorter SSW TOF in the former case. This apparent contradiction indicates strongly that the increase in the pressure, density, and temperature in the case of the Cu wire array explosion is related to the additional energy delivered to the converging SSW by the SSW reflected from the reflector. This qualitative explanation agrees with the simulation results of the pressure distributions at different times of the converging SSW implosion shown in Figure 8 for the Al wire array explosion without the reflector and for the Cu wire array explosion with and without the reflector.

Simulations of the Al wire array explosion with experimentally measured energy density deposition (even for $\alpha = 1$) and the SESAME database for Al showed a value for the SSW's TOF that is significantly larger than the TOF value measured in the experiment. In order to fit the experimental data, one has to consider additional energy deposited into the water flow by the Al wire array explosion which, in our case, could be the energy realized by the Al wire's combustion.

Indeed, one can see that, in spite of the fact that the SSW generated by the Al wire array explosion arrives earlier at $r \approx 0.15$ mm than the primary SSW generated by the

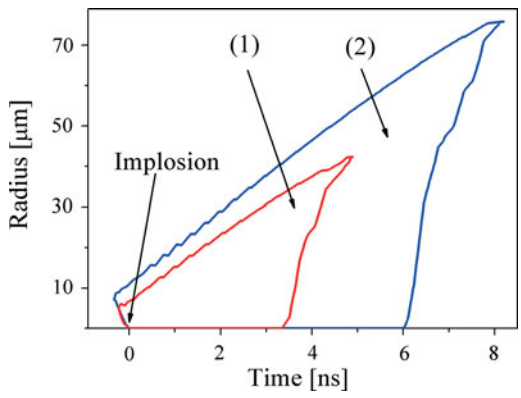

Fig. 7. (Color online) Time evolution of the radial position of a 100 GPa pressure in water generated SSW in Cu wire array underwater electrical explosion. (**1**) and (**2**) are the cases without and with external duralumin reflector.

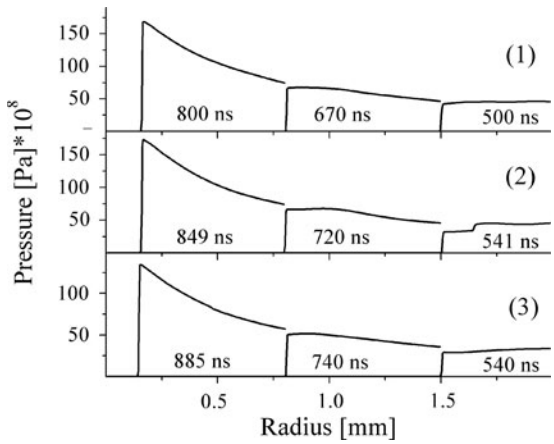

Fig. 8. Simulated radial distribution of the pressure behind converging SSW at different times of implosion: (**1**) Al wire array without the reflector, (**2**) Cu wire array with the reflector, and (**3**) Cu wire array without the reflector. The presented profiles correspond to the positions of the SSW front at radii of 1.5 mm, 0.8 mm, and 0.15 mm at times shown in the figure.

Cu wire array explosion, the pressure in the vicinity of the implosion axis ($r = 2.5$ μm) is larger in the latter case due to the additional energy delivered by the reflected SSW (see Table 2).

In the case of Al wire array explosion, additional energy deposited into the converging water flow results due to the combustion of the Al wires. The maximal amount of energy release related to the Al's combustion can be calculated as (Kortchondziya *et al.*, 1999):

$$2\mathrm{Al}\ (solid) + 3\mathrm{H_2O}\ (liquid) = \mathrm{Al_2O_3}\ (solid) + 3\mathrm{H_2}\ (gas) + \mathrm{Q(15kJ/g)}. \quad (4)$$

In the set of experiments presented here, the total mass of the Al wires was 0.03 g, which theoretically results in an additional energy of $W_{comb} = 450$ J in the case of Al wires complete combustion. The experimental data (see Tables 1) show that when an Al wire array is used, the time of the SSW implosion is significantly decreased. This SSW additional acceleration can be related only to the combustion of the Al wires. In order to fit experimental data, results of 1D HD simulations showed that the additional energy deposited into the converging water flow should be about 200 J. In this case, the maximum pressure, density, and temperature of water at $r = 2.5$ μm are increased by 34%, 7%, and 33%, respectively, in comparison with Cu wire array explosion (without the reflector).

The same as in the case of the Cu wire array explosions, application of the reflector in the case of Al wire array explosion results in additional energy of about 170 J delivered to the converging water flow by the reflected SSW. However, in the case of Al wire array explosion, the application of the reflector leads to only an 11%, 2%, and 9% relative increase in values of pressure, density and temperature, respectively, as compared with those values obtained with Al wire array explosion without the reflector. The latter is explained by Al combustion, which results in an additional about 200 J being delivered to the water flow.

To conclude, one obtains that Al wire array (5 mm in diameter) explosion with the reflector allows one to obtain an additional increase in the pressure, density, and temperature at $r = 2.5$ μm of 48%, 9%, and 46%, respectively, as compared with the case of Cu wire array explosion without the reflector using almost the same deposited energy into the exploding wire array.

4.2. Optimization of the Reflector Position

The experimental and simulation results showed that the decrease in the SSW TOF and, respectively, the increase in the values of pressure, temperature, and density of water in the vicinity of the implosion axis is obtained only when the reflector is made of a material, with a density value that is significantly greater than that of water, and when the reflector is placed close to the wire array. The first optimization condition follows from the reflection law, which requires one to use a reflector material whose mass density is much higher than water density, in order to obtain the largest value of the reflection coefficient. This dictates the use of metals or their alloys, which are simultaneously resistant to shocks. The second optimization condition requires that the reflected SSW arrives at the implosion axis with as small as possible a delay behind the primary converging SSW, and that no breakdown to reflector occurs. Optimization of these two conditions allows one to achieve maximal value of pressure in the vicinity of implosion axis. Here let us note that one cannot install the reflector in the vicinity of the wire array because of the electrical breakdown that would occur between the exploding wire and the conducting reflector. Therefore, a set of simulations was performed in order to find the optimal distance between the wires and reflector when using duralumin as the reflector material. In addition, simulations were performed that considered different rates of energy deposition while keeping the total deposited energy value the same. Namely, in these simulations, the full width half maximum durations of the power deposition were 150, 300, and 600 ns in order to obtain the optimal reflector diameter for pulsed generators having 200, 400, and 800 ns current rise times and, respectively, different rates of energy deposition (Bazalitsky *et al.*, 2011). It should be mentioned that in the case of a 5 mm and 10 mm array radius, for a 400 ns discharge current rise time the energy deposition was obtained experimentally. The results of these simulations for explosions of wire arrays being 5 mm and 10 mm in diameter are shown in Figure 9. One can see that in order to obtain the highest pressure in the vicinity of the implosion axis, the optimal value of Δr for wire arrays with different diameters is almost not affected by the current rise time and is equal to 0.2 mm and about 0.45 mm for wire arrays with a diameter of 5 mm and 10 mm, respectively. In fact, the effect of the reflector on the pressure in the vicinity

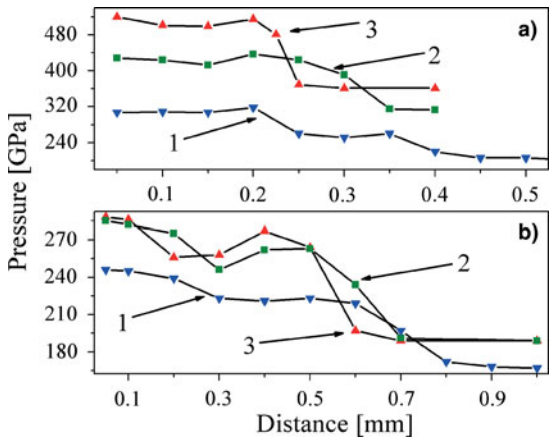

Fig. 9. (Color online) Dependence of the maximal value of the pressure at r=2.5 μm versus the distance between the Cu wire array and the reflector for different energy deposition times. (**a**) and (**b**) for the array diameters of 5 mm and 10 mm, respectively. Discharge current rise time is: (**1**) 800 ns, (**2**) 400 ns, and (**3**) 200 ns.

of the implosion axis can be noticed also at distances Δr greater than the optimal, and it is changes as a function of current rise time. In addition, one can see that the faster the rise time of the discharge current and, respectively, the shorter the full width half maximum of the deposited energy, the smaller is the distance Δr required to obtain an increase in the SSW pressure at $r \leq 2.5$ μm. This is explained by a faster SSW propagation toward the implosion axis when the energy deposition rate is faster. An increase in the diameter of the wire array allows one to increase also the value of Δr. However, in this case a smaller resultant pressure is obtained at $r \leq 2.5$ μm than when the diameter of the wire array is smaller for the same energy deposition rate.

In addition, a set of 1D HD simulations of Cu wire array explosion was performed using different specific mass densities of the reflector material. Here again, HD simulations were coupled to the SESAME database of equation of states. The purpose of these simulations was to find the dependence of the energy reflected from the reflector toward the implosion axis on the specific density of the reflector material's mass. It was found that this dependence is in good agreement with theoretical estimates based on mass and momentum conservation laws. The dependence of the efficiency of the transfer of the energy deposited into the exploding wire to the converging water flow on the mass specific density of the reflector placed at the optimal distance from the wire array is shown in Figure 10. In these simulations, the rate of energy deposition into the wires was equal to the experimental data obtained in a typical explosion of a Cu wire array with a diameter of 5 mm. One can see that there is no significant improvement in the efficiency value when the reflector's material has a mass density higher than about 7 g/cm^3. These simulation results agrees with experimental data showing that the fastest SSW TOF (795 ± 5 ns) is obtained in the Al wire array (5 mm in diameter) explosion with a reflector made of stainless steel. Following experimental data, simulations showed that the pressure and density of water at $r = 2.5$ μm to be 536 GPa and 4.23 g/cm^3, respectively. The latter exceeds the pressure and density of water in the case of Cu wire array explosion without the reflector in 67% and 12%, respectively.

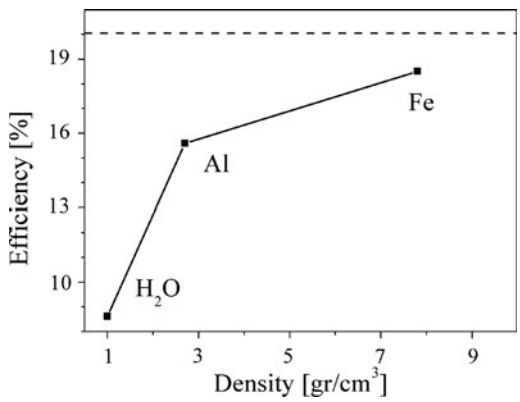

Fig. 10. Efficiency of the energy deposition to the converging water flow versus mass specific density of reflector material for the case of Cu wire array with a diameter of 5 mm. The dashed line corresponds to the SSW reflection from a reflector with infinitely high density.

4.3. Second Light Emission Pulse

Recent results (Fedotov-Gefen *et al.*, 2011) for water self-light emission obtained in experiments with a microsecond timescale of wire array explosions showed that an intense and short-duration radiation pulse when the SSW arrives at the implosion axis is followed by a second light emission pulse. The latter is delayed with respect to the first light emission pulse by 1–2 μs and it is of significantly larger time duration ($>10^{-6}$ s). In Fedotov-Gefen *et al.* (2011), it was considered that a possible reason for the second emission pulse is the compression of the "water plasma" by the SSW reflected from the exploded wire array. However, the results of our modified 1D HD simulation showed that the SSW reflected from the exploded and expanded wire array has a negligibly small effect on the pressure in the vicinity of the implosion axis. Thus, the appearance of the second light emission is not governed by the SSW reflected from the Cu layer. The same simulations results showed that the time of the beginning of the second light emission pulse is in good agreement with the time when water reaches its binodal state, which is accompanied by the rapid formation of bubbles. The generation of bubbles causes a drastic increase in the scattering of the light that is continuously emitted by the exploded Cu wires (Grinenko *et al.*, 2006; Veksler *et al.*, 2009). This scattered light is obtained as the second light emission pulse. This explanation was experimentally proven in experiments with the same wire array explosion but with a non-transparent black dielectric tube about 8 mm in diameter, installed co-axially inside the array. These experiments showed the same first short duration emission pulse as without the tube, and the absence of the second light emission pulse.

In Figure 11a, one can see the waveform of the second light emission pulse obtained in experiments with a Cu wire array (10 mm in diameter) explosion. The result of the 1D HD simulations for this explosion, using the values of energy density deposition into the wire array that had been measured experimentally, showing radial dependence of the water reaching binodal state versus time, is presented in Figure 11b. These simulations showed that the formation of water in the binodal state occurs due to two processes. On the one hand, when the SSW reflected from the implosion axis reaches the "Cu layer," the density of which at that time is smaller than the density of the water behind the SSW front, one obtains formation of the rarefaction wave, which propagates towards the implosion axis. On the other hand, the pressure and density of the water behind the SSW reflected from the axis decreases rather fast and at time $t > 3.6$ μs (see Fig. 11b) one obtains conditions for the binodal state of water almost simultaneously up to a radius of 3 mm.

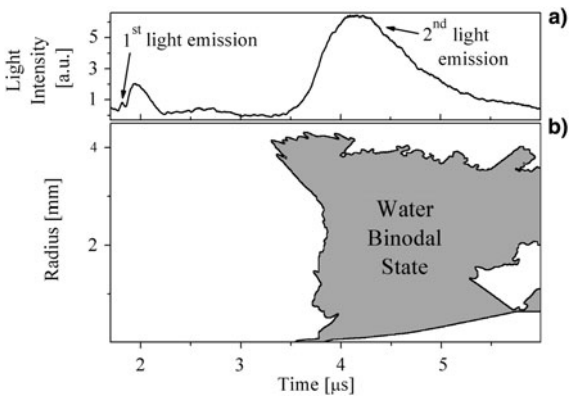

Fig. 11. (**a**) First and second light emission pulse obtained by the PMT coupled with 656 nm interference filter in experiment with Cu wire array explosion. (**b**) Result of 1D HD simulation with experimentally obtained energy deposition showing formation of bubbles versus time. Dashed area corresponds to the pressure and temperature where the water is in the vapor phase. The time "0" corresponds to the beginning of the discharge current.

5. SUMMARY

Experimental research and 1D HD simulations showed that application of a reflector made of a material whose density is significantly larger than that of water, placed outside the exploding wire array, allows one to increase the efficiency of the transfer of the energy deposited into the wires to the converging water flow and, respectively, to increase the values of pressure, density, and temperature of water in the vicinity of the implosion axis. Namely, experiments with a duralumin reflector showed that at $r = 2.5$ μm the values of pressure, density, and temperature increase by 38%, 7%, and 33%, respectively, in the case of Cu wire array. An additional increase in water density, pressure, and temperature in the vicinity of the implosion axis can be achieved using an Al wire array explosion with reflector made of stainless steel. In this case, the maximum pressure and density at $r = 2.5$ μm are increased by 76% and 12%, respectively, as compared with Cu wire array explosion without the reflector due to additional energy delivered to the converging water flow during Al combustion and by reflected SSW.

Finally, experiments carried out with the explosion of Cu wire arrays, with and without a dielectric tube that is not transparent for visible light installed inside the exploding wire array, and 1D HD simulations showed that the second light emission pulse is related to the formation of bubbles because of the water boiling at the time when the pressure decreases below critical value and the water reaching its binodal state.

REFERENCES

Bazalitski, G., Gurovich, V.Tz., Fedotov-Gefen, A., Efimov, S. & Krasik, Ya.E. (2011). Simulation of converging cylindrical GPa-range shock waves generated by wire array underwater electrical explosions. *Shock Waves* **21**, 321–329.

Celliers, P.M., Collins, G.W., Hicks, D.G., Koenig, M., Henry, E., Benuzzi-Mounaix, A., Batani, D., Bradely, D.K., Da Silva, L.B., Wallace, R.J., Moon, S.J., Eggert, J.H., Lee, K.K.M., Benedetti, L.R., Jeanloz, R., Masclet, I., Dague, N., Marchet, B., Rabec, Le Gloahec, M., Reverdin, Ch., Pasley, J., Willi, O., Neely, D. & Danson, C. (2004). Electronic conduction in shock-compressed water. *Phys. Plasmas* **11**, L41–L44.

Efimov, S., Gurovich, V.Tz., Bazalitski, G., Fedotov, A. & Krasik, Ya.E. (2009). Addressing the efficiency of the energy transfer to the water flow by underwater electrical wire explosion. *J. Appl. Phys.* **106**, 073308/1–8.

Fedotov, A., Grinenko, A., Efimov, S. & Krasik, Ya.E. (2007). Generation of cylindrically symmetric converging shock waves by underwater electrical explosion of wire array. *Appl. Phys. Lett.* **90**, 201502/1–3.

Fedotov-Gefen, A., Efimov, S., Gilburg, L., Bazalitski, G., Gurovich, V.Tz. & Krasik, Ya.E. (2011). Generation of a 400GPa pressure in water using converging strong shock waves. *Phys. Plasmas.* **18**, 062701/1–8.

Fedotov-Gefen, A., Efimov, S., Gilburg, L., Gleizer, S., Bazalitsky, G., Gurovich, V.Tz. & Krasik, Ya.E. (2010). Extreme water state produced by underwater wire-array electrical explosion. *Appl. Phys. Lett.* **96**, 221502/1–3.

Goldman, N., Reed, E.J., Kuo, I.F., Fried, L.E., Mundy, C.J. & Curioni, A. (2009). Ab initio simulation of the equation of state and kinetics of shocked water. *J. Chem. Phys.* **130**, 124517/1–6.

Grinenko, A., Efimov, S., Fedotov, A., Krasik, Ya.E. & Shnitzer, I. (2006). Efficiency of the shock wave generation caused by underwater electrical wire explosion. *J. Appl. Phys.* **100**, 113509/1–8.

Grinenko, A., Gurovich, V.T. & Krasik, Ya.E. (2007). Implosion in water medium and its possible application for the inertial confinement fusion. *Phys.Plasmas.* **14**, 012701/1–7.

Grinenko, A., Krasik, Ya.E., Efimov, S., Fedotov, A., Gurovich, V.Tz. & Oreshkin, V.I. (2006). Nanosecond time scale, high power electrical wire explosion in water. *Phys. Plasmas* **13**, 042701/1–14.

Kalitkin, N.N. (1978). *Numerical Methods*. Moscow: Nauka.

Kolacek, K., Prukner, V., Schmidt, J., Frolov, O. & Straus, J. (2010). A potential environment for lasing below 15 nm initiated by exploding wire in water. *Laser Part. Beams* **28**, 61–67.

Kortchondziya, V.P., Mdivnishvili, V.P. & Taktakishvili, M.I. (1999). About generation of pulsed pressure in liquid by the use of metallic plasma and measurements of some of characteristics of the pressure. *J. Techn. Phys.* **69**, 41–43.

Kovalchuk, B.M., Kharlov, A.V., Zorin, V.B. & Zherlitsyn, A.A. (2009). A compact submicrosecond, high current generator. *Rev. Sci. Instr.* **80**, 083504/1–6.

Krasik, Ya.E., Grinenko, A., Sayapin, A. & Gurovich, V.Tz. (2007). Generation of sub-Mbar pressure by converging shock waves produced by the underwater electrical explosion of a wire array. *Phys. Rev. E.* **73**, 057301/1–4.

Lindl, J. (1995). Development of the indirect-drive approach to inertial confinement fusion and the target physics basis for ignition and gain. *Phys. Plasmas.* **2**, 3933–4024.

Lyon, S.P. & Johnson, J.D. (1992). SESAME: The Los Alamos National Laboratory, Report No LA-UR-92-3407.

Mitchell, A.C. & Nellis, W.J. (1981). Diagnostic system of the Lawrence Livermore National Laboratory two-stage light-gas gun. *Rev. Sci. Instrum.* **52**, 347–360.

Nellis, W.J., Holmes, N.C., Mitchell, A.C., Hamilton, D.C. & Nicol, M. (1997). Equation of state and electrical conductivity

of "synthetic Uranus," a mixture of water, ammonia, and isopropanol, at shock pressure up to 200GPa (2Mbar). *J. Chem. Phys.* **107**, 9096–9100.

Sasaki, T., Yano, Y., Nakajima, M., Kawamura, T. & Horioka, K. (2006). Warm-dense-matter studies using pulse-powered wire discharges in water. *Laser Part. Beams* **24**, 371–380.

Spielman, R.B., Deeney, C., Chandler, G.A., Douglas, M.R., Fehl, D.L., Matzen, M.K., McDaniel, D.H., Nash, T.J., Porter, J.L., Sanford, T.W.L., Seamen, J.F., Stygar, W.A., Struve, K.W., Breeze, S.P., McGurn, J.S., Torres, J.A., Zagar, D.M., Gilliland, T.L., Jobe, D.O., McKenney, J.L., Mock, R.C., Vargas, M., Wagone, T. & Peterson, D.L. (1998). Tungsten wire-array Z-pinch experiments at 200 TW and 2 MJ. *Phys. Plasmas* **5**, 2105–2111.

Tahir, N.A., Stöhlker, Th., Shutov, A., Lomonosov, I.V., Fortov, V.E., French, M., Nettelmann, N., Redmer, R., Piriz, A.R., Deutch, C., Zhao, Y., Xu, H., Xiao, G. & Zhan, W. (2010). Ultrahigh compression of water using intense heavy ion beams: Laboratory planetary physics. *New J. Phys.* **12**, 073022/1–17.

Veksler, D., Sayapin, A., Efimov, S. & Krasik, Ya.E. (2009). Characterization of Different Wire Configurations in Underwater Electrical Explosion. *IEEE Trans. Plasma Sci.* **37**, 88–98.